

# Single-Walled Carbon Nanotubes Shell Decorating Porous Silicate Materials: A General Platform for Studying the Interaction of Carbon Nanotubes with Photoactive Molecules

Avishek Saha,<sup>a,c</sup> Saunab Ghosh,<sup>a,c</sup> Natnael Behabtu,<sup>c,d</sup> Matteo Pasquali,<sup>a,c,d</sup> Angel A. Martí<sup>a,b,c,\*</sup>

<sup>a</sup>Department of Chemistry, <sup>b</sup>Department of Bioengineering, and <sup>c</sup>Department of Chemical and Biomolecular Engineering, Rice University, 6100 Main Street, Houston TX 77005.

<sup>d</sup>Richard E. Smalley Institute for Nanoscale Science and Technology, Rice University, Houston, Texas 77005

## Supporting Information

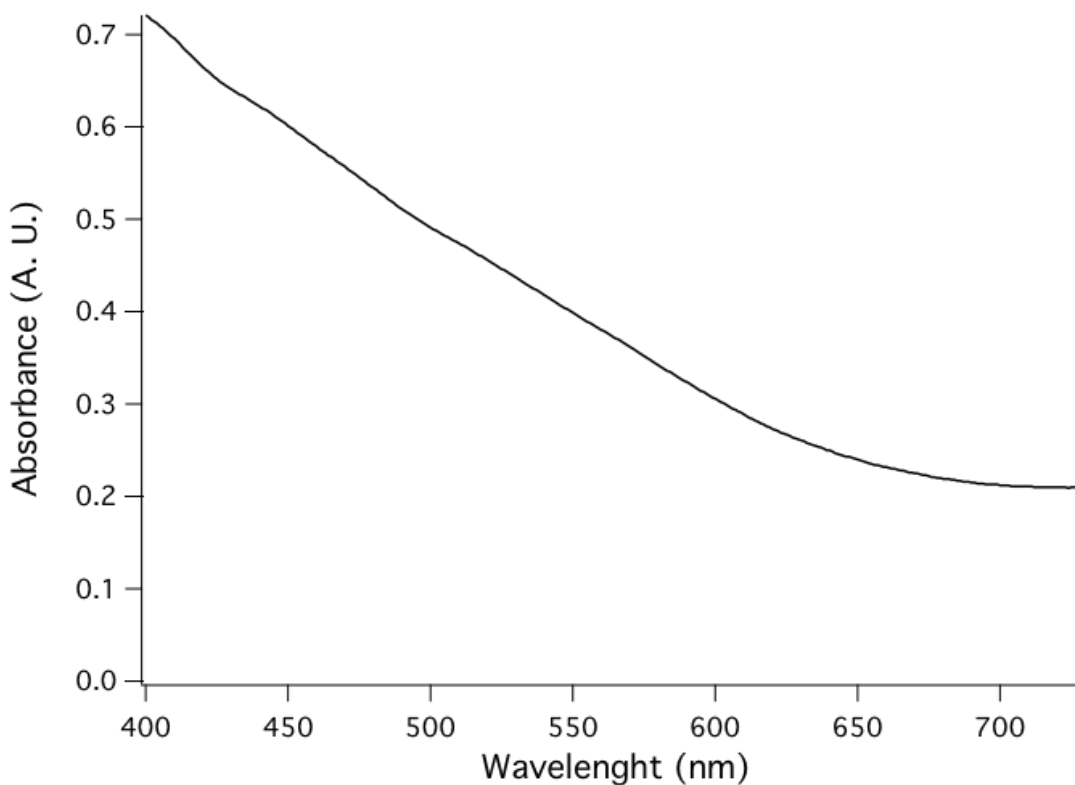


**Figure S1.** UV-Vis spectrum of SWCNTs dissolved in CSA. The absence of van Hove transitions is noticeable.

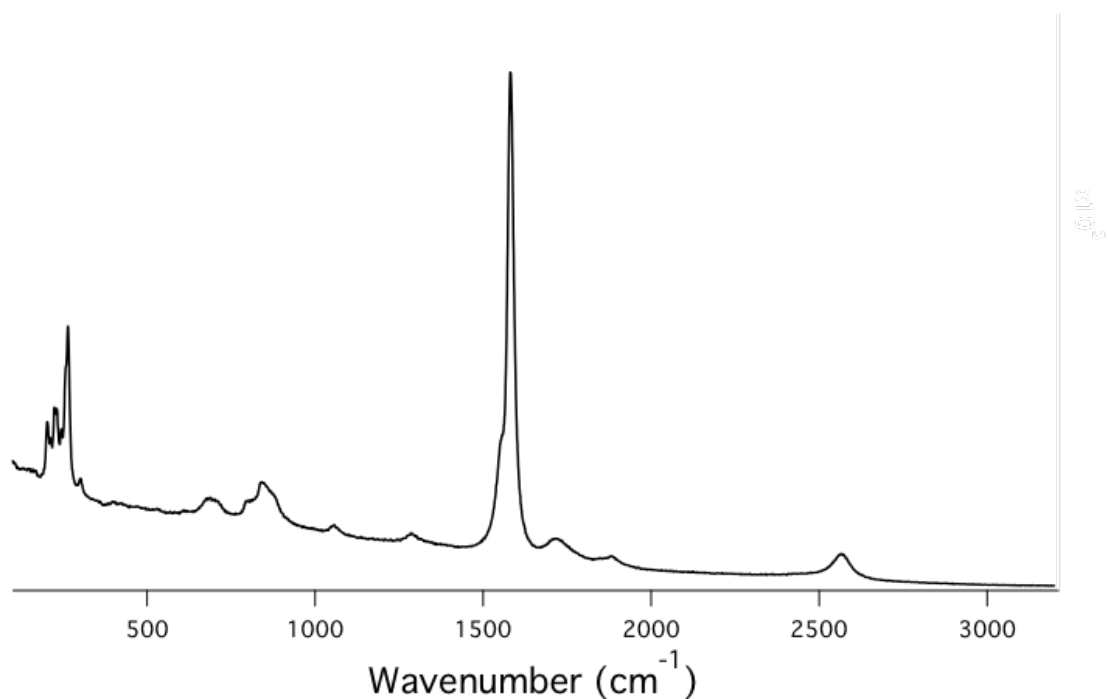


**Figure S2.** Raman spectrum of SWCNTs crashed out of MCM-41-A by addition of ethyl ether. The Raman spectrum of SWCNTs extracted from MCM-41-A this way shows the recovery of the roping peak. Moreover, this Raman spectrum is practically indistinguishable from the Raman spectrum of the pristine bundled SWCNTs powder shown in Figure 2b.

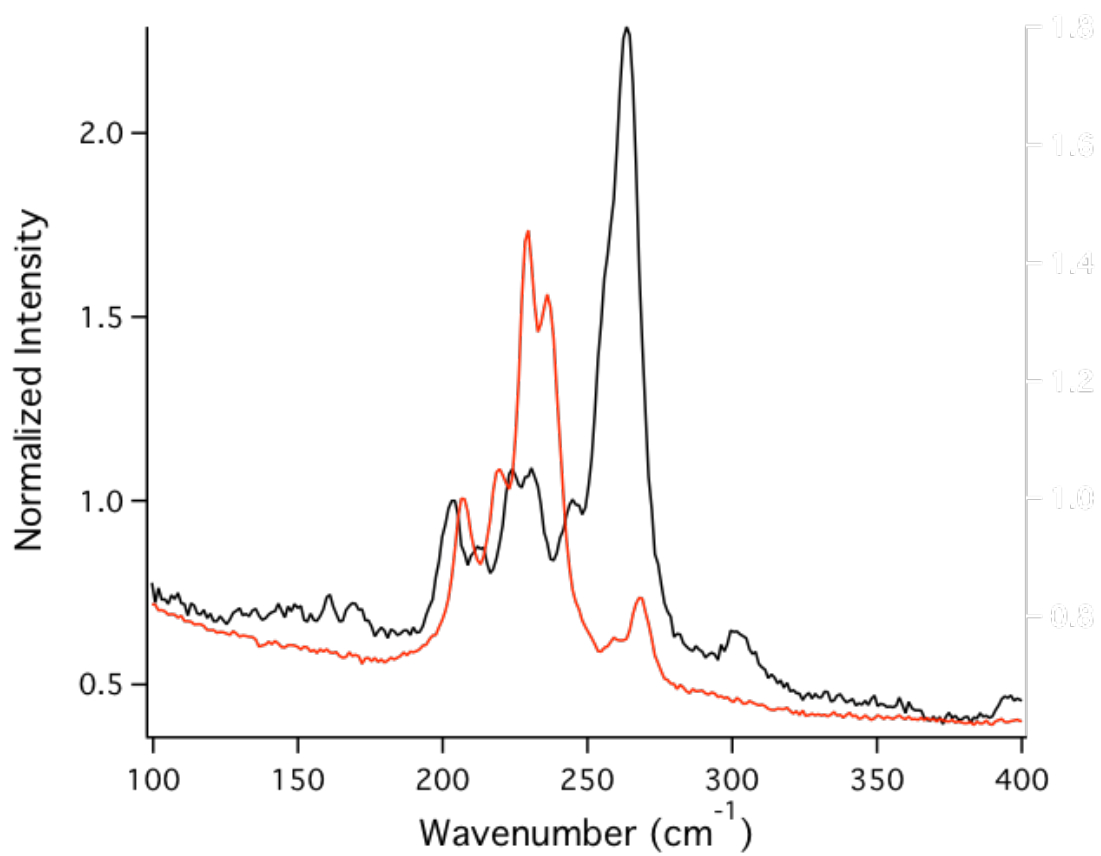


**Figure S3.** Expanded Raman spectra of the RBM region for pristine SWCNTs (—) and vpSWCNTs@MCM-41 (—).

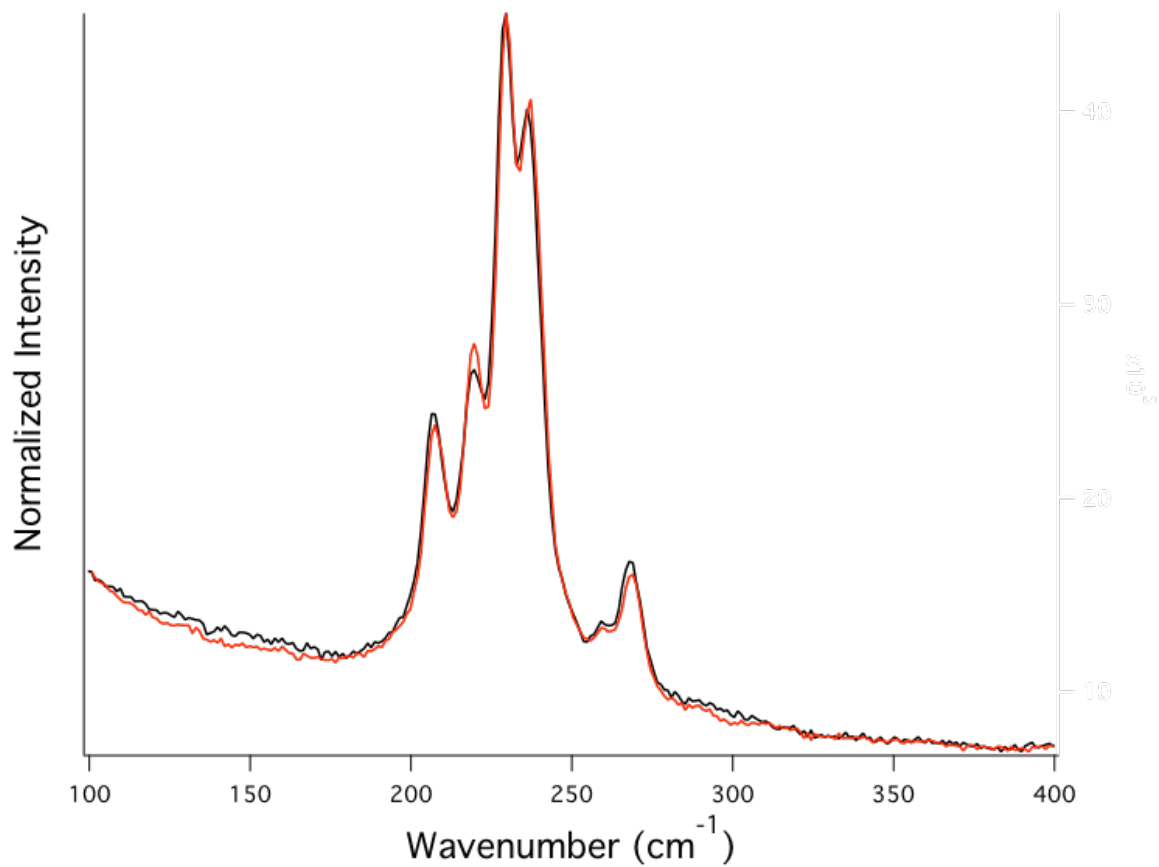


**Figure S4.** Expanded Raman spectra of the RBM region for vpSWCNTs@MCM-41 0.67% (w/w) (—) and vpSWCNTs@MCM-41 1.3% (w/w) (—). The roping peak at 261 cm<sup>-1</sup> does not change significantly.

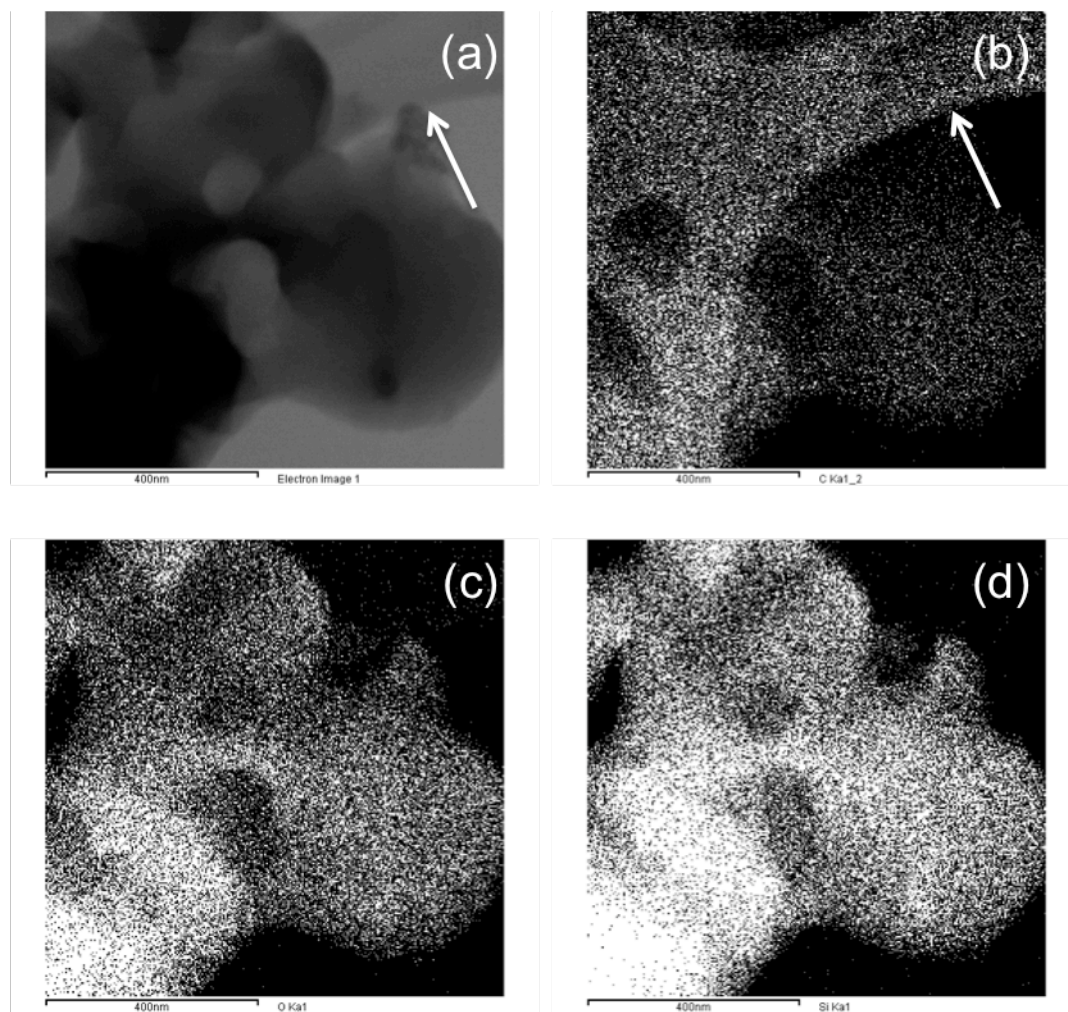


**Figure S5.** (a) TEM image of a MCM-41 particle on a Lacey Formvar grid (carbon coated). The arrow points to the Formvar grid. EDS elemental mapping showing the distribution of (b) carbon, (c) oxygen, and (d) silicon. Strong oxygen and silicon signals are observed coming from the MCM-41 but not from the Formvar grid. Carbon signals can be seen coming from the Formvar and also from the MCM-41 particle. The homogeneous distribution of carbon is indicative of a good dispersion of the SWCNTs the particle.

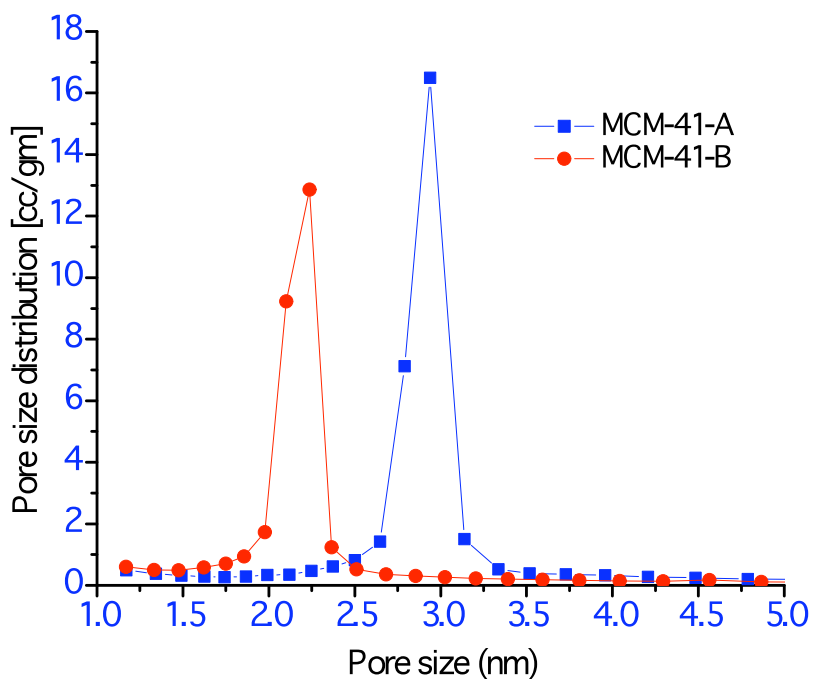
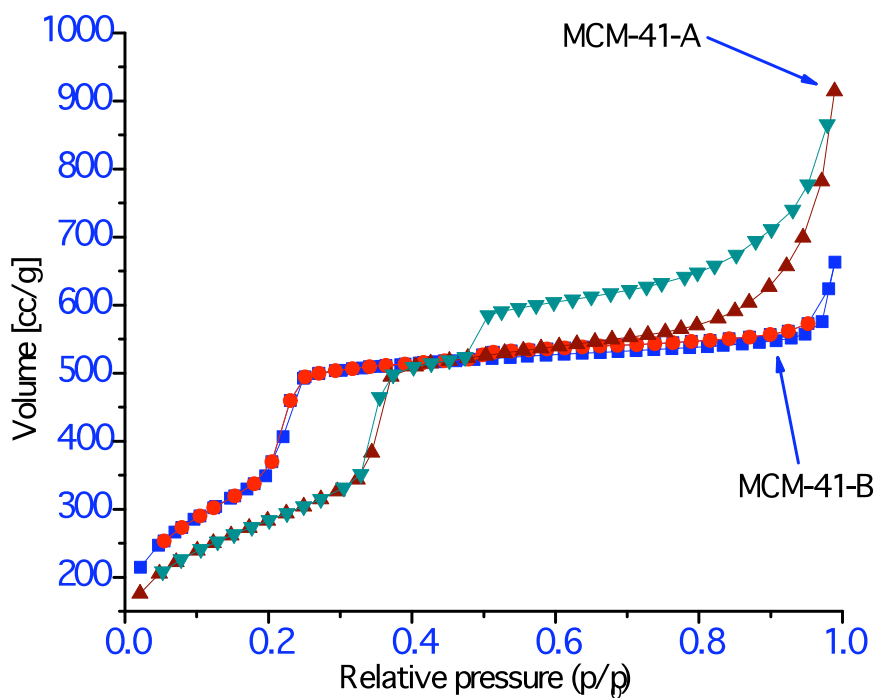


**Figure S6.** Nitrogen adsorption isotherms and pore size distributions of MCM-41 samples. Nitrogen adsorption measurements were performed at 77 K on an Autosorb AS-3B adsorption analyzer. Both samples were outgassed at 473 K for 18 h before

measurements. The characteristic feature of sharp capillary condensations is clearly discernible (top of Fig S6) for both MCM-41-A and MCM-41-B samples. However the position of condensation steps shifted to higher relative pressure in case of MCM-41-A due to slight difference in mesopore sizes (than MCM-41-B). As we can see in pore size distributions (calculated using BJH method), the pore sizes of MCM-41-A and MCM-41-B are 2.9 and 2.2 nm respectively.

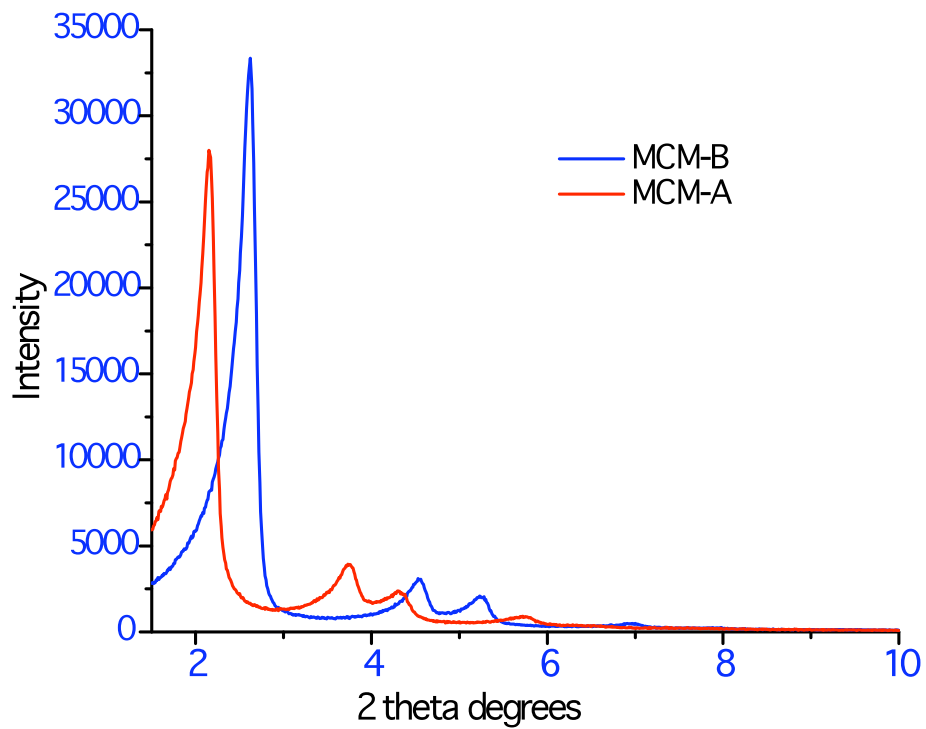


**Figure S7.** Powder XRD patterns of MCM-41 samples.

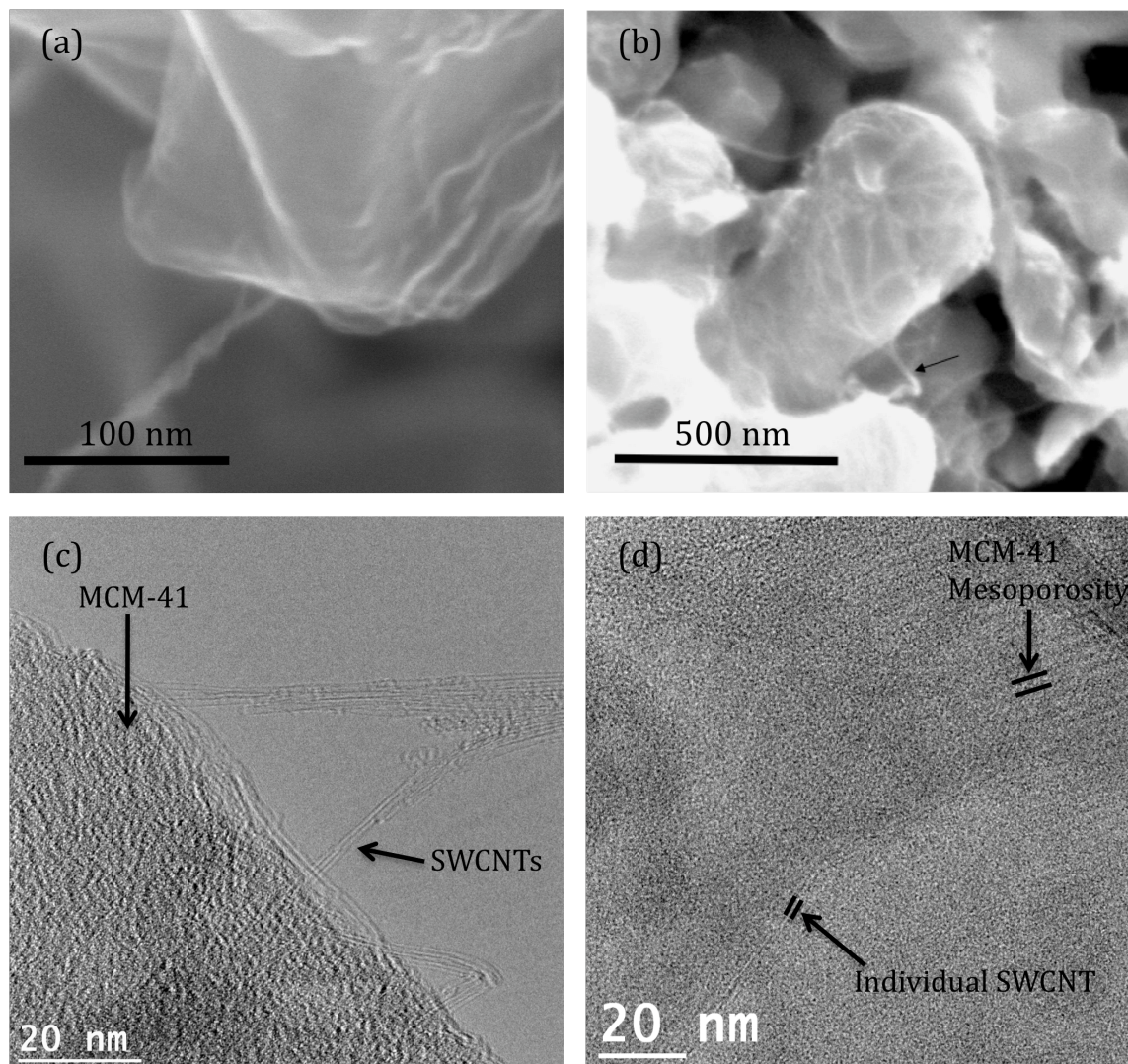


**Figure S8.** SEM images of (a) pSWCNTs@NaY zeolite, and (b) pSWCNTs@MCM-41. (c) and (d) HR-TEM images of SWCNTs on the surface of MCM-41.

Although it would be reasonable to think that pSWCNTs in the surface of silicate materials are mostly individualized due to the electrostatic repulsion among their protonated walls, we tried to assess the degree of individualization using imaging techniques such as SEM and TEM. Figure S8a shows the SEM of pSWCNTs-NaY; individual SWCNTs are difficult to distinguish on the surface of the silicate materials, and can be mostly distinguished when they protrude out of their surface. In this image intertwined SWCNTs departing from the surface of NaY can be seen. Figure S8b shows a lower magnification image of pSWCNTs-MCM-41 in which complete coverage of the particle by SWCNTs is observed. All of the structures seen in Figure S8a and b are less than 15 nm in diameter, indicating that small bundles can be found. This contrast with bundles of hundreds of nanometers found for pristine purified SWCNTs materials. Nevertheless, this doesn't rule out that a large population of pSWCNTs are individual. It is more likely that individual SWCNTs are below the resolution of the SEM instrument used to monitor our samples (HiPco SWCNTs have diameters from 0.8 to 1.2 nm). Therefore, bundled structures, which have larger diameters, stick out on the images since their larger sizes are within the SEM resolution.

In order to achieve a better resolution, microscopy images using HR-TEM were obtained. TEM however present two challenges: (1) low Si/C contrast and (2) it is difficult to adjust the focal plane to the surface of non-planar objects. Despite these limitations we were able to see some images where small bundles and individual SWCNTs are observed. Figure S8c shows two small bundles departing from the surface of MCM-41. Figure S8d shows an individual pSWCNTs on the surface of MCM-41 (0.8 nm diameter) and even some of the material mesoporosity (pore size ca. 2.7 nm). Together, SEM and TEM images also show that rope formation is favored when SWCNTs detach from the silicate surface (Figure S8). We speculate that aggregation is mostly inhibited when the SWCNTs are on the surface of MCM-41, but favorable if the nanotubes find each other when standing apart from the surface.

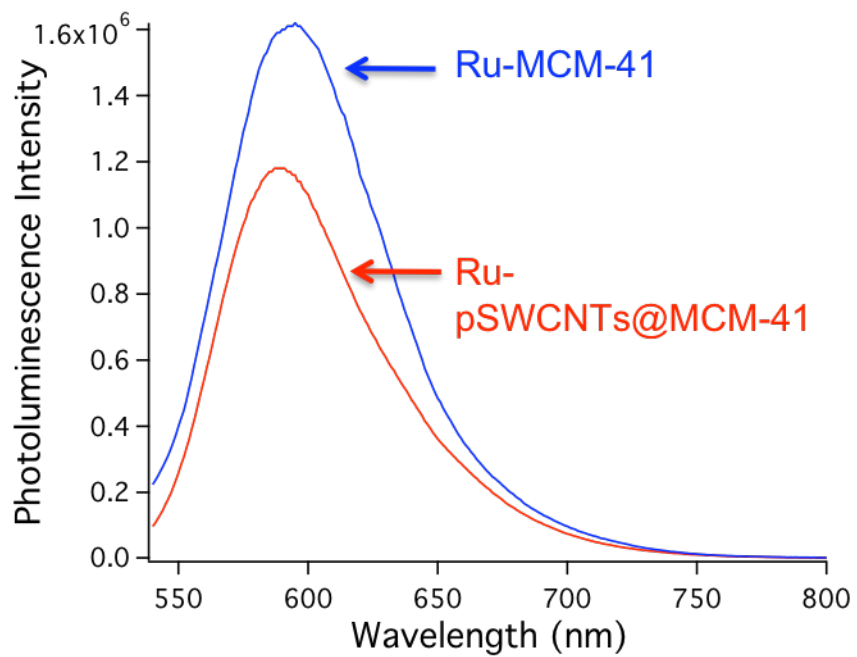


**Figure S9.** Photoluminescence spectra for Ru-MCM-41 and Ru-pSWCNTs@MCM-41.

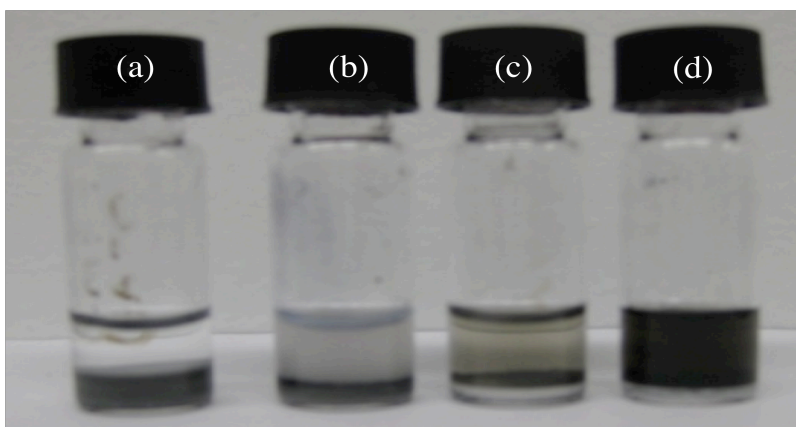


**Figure S10.** Photographs of surfactant dispersed SWCNTs in (a) 1% DTAB solution with MCM-41; (b) 1% pluronic-F68 solution with MCM-41; (c) 1% DTAB solution with NaY; (d) 1% pluronic F-68 solution with NaY. Images were taken after stirring the surfactant dispersed SWCNTs solution with the respective scaffolds material for 24 hours. Nanotubes are crashing out of solution forming heterogeneous layer on the MCM-41 or NaY. The images show a white powder (zeolite or MCM-41) on the bottom of the flask, generally covered with a layer of black powder (SWCNTs). The two layers can be distinguished more easily for (c) and (d).